An Exact Expression for Multidimensional Spectroscopy of a Spin-Boson Hamiltonian

Albert Liu

Multidimensional coherent spectroscopy is a powerful tool to characterize nonlinear optical response functions. Typically, multidimensional spectra are interpreted via a perturbative framework that straightforwardly provides intuition into the density matrix dynamics that give rise to specific spectral features. When the goal is to characterize system coupling to a thermal bath however, the perturbative formalism becomes unwieldy and yields less intuition. Here, an approach developed by Vagov et al. is extended to provide an exact expression for multidimensional spectra of a spin-boson Hamiltonian up to arbitrary order of electric field interaction. The utility of this expression is demonstrated by modeling polaron formation and coherent exciton-phonon coupling in quantum dots, which strongly agree with experiment.

1. Introduction

Many quantum systems of both fundamental and practical interest may be considered open quantum systems,[1] in which relevant degrees of freedom (the 'system') are coupled in some significant way to a thermal environment (the 'bath'). In recent years, the interaction between the system and the bath has become a topic of increasing interest to varied communities.[2,3] This is driven by two primary motivations, namely that system-bath coupling is essential to understanding complex quantum systems[4,5] and that optimizing thermal decoherence is essential for quantum technologies.[6–8]

Optical spectroscopy is perhaps the most direct way of interrogating open quantum systems. Most commonly, linear spectroscopies such as absorption or fluorescence spectroscopy[9] return spectral lineshapes that provide insight into coherence dephasing, and thereby system-bath coupling.[10,11] These methods fail in the presence of disorder however, where an inhomogeneous resonance energy distribution obscures the homogeneous lineshapes. In response to this challenge, nonlinear spectroscopic techniques were developed to extract homogeneous lineshapes even in the presence of dominant disorder. For example, photon echo spectroscopy[12] and spectral hole burning[13] are two such nonlinear spectroscopies that have been widely applied to

a variety of atomic,[14,15] molecular,[16] and solid-state[17,18] systems.

Undoubtedly the most general nonlinear spectroscopic technique is multidimensional coherent spectroscopy (MDCS).[19,20] An optical analogue of nuclear magnetic resonance, MDCS involves impulsive excitation of a system by a sequence of laser pulses and measurement of the resultant nonlinear wave-mixing signal.[21] Dynamics of the system density matrix are encoded in the inter-pulse time-delays,[22] and Fourier transform of the nonlinear signal along two or more of the experimental time axes returns a multidimensional spectrum that contains a wealth of information about the microscopic physics. Multidimensional spectra are typically interpreted perturbatively,[20,22] in which electric field interactions induce sequential changes in the system density matrix, which provides clear intuition for the coherent and incoherent dynamics that evolve across various time axes.[23,24] However, the formalism becomes cumbersome upon incorporating system-bath coupling, particularly for higher-order nonlinearities.[25,26]

Here, we present an exact, non-perturbative expression for multidimensional spectroscopy of a spin-boson Hamiltonian, a ubiquitous model for open quantum systems. While not generally applicable to all quantum systems, most material platforms relevant to quantum technologies can be reduced to such a description. Derived from a treatment developed by Vagov et al.,[27] the compact expression presented here provides a way to more easily model many complex systems and interpret their spectra. We demonstrate its utility by reproducing experimental signatures of polaron formation and coherent exciton-phonon coupling in quantum dots.

2. Spin-Boson Hamiltonian

Specifically, the model we consider is that of a spin-boson Hamiltonian[28–30] without tunneling, often termed in the literature as the 'independent boson Hamiltonian'.[31] This consists of a (electronic) two-level 'system', a collection of (vibrational) harmonic oscillators that comprise the 'bath', and coupling between the two is retained to lowest order (bi-linearly). For ease of comparison, we use the notation of [27] and the Hamiltonian reads:

$$H = \hbar\Omega c^\dagger c + \sum_{q,i} \hbar\omega_{q,i} b^\dagger_{q,i} b_{q,i} - (MEc^\dagger d^\dagger + M^* E^* dc)$$

$$+ \sum_{q,i} \hbar\left[(g^e_{q,i} b_{q,i} + g^{e*}_{q,i} b^\dagger_{q,i})c^\dagger c - (g^h_{q,i} b_{q,i} + g^{h*}_{q,i} b^\dagger_{q,i})d^\dagger d \right] \quad (1)$$

A. Liu
Condensed Matter Physics and Materials Science Division
Brookhaven National Laboratory
Upton, New York 11973, USA
E-mail: aliu1@bnl.gov

The ORCID identification number(s) for the author(s) of this article can be found under https://doi.org/10.1002/qute.202300399

**ADVANCED
SCIENCE NEWS**

www.advancedsciencenews.com

**ADVANCED
QUANTUM
TECHNOLOGIES**

www.advquantumtech.com

where $c^{(\dagger)}$, $d^{(\dagger)}$, and $b_{\mathbf{q}}^{(\dagger)}$ are the (creation) annihilation operators for electrons, holes, and a vibrational mode of wavevector $\mathbf{q}$ and branch index i respectively. In order, $\hbar\Omega$ is the electronic energy splitting, $\hbar\omega_{\mathbf{q},i}$ is the energy of the respective vibrational mode, M is the electronic dipole moment that interacts with an external electric field $E(t)$, and $g_{\mathbf{q},i}^{(e)h}$ is the coupling strength between the (electrons) holes and each vibrational mode. From here on we assume a single branch and eliminate the branch index i, though all equations can be generalized to multiple branches by re-introducing i to the wavevector index. Note that from a classical perspective, the final coupling term shifts the vibrational coordinate of minimum energy upon electronic excitation, which results in the displaced oscillator model for a single mode.

2.1. Spectral Density

The effects of system-bath coupling may be captured in a quantity termed the spectral density $C''(\omega_\nu)$,[29,32,33] which resolves the coupling strength as a function of vibrational frequency ω_ν. Here, we first consider a Debye contribution[34] to the spectral density at low frequencies, a common functional form used to model a variety of cases ranging from molecular systems[35] to quantum dots:[36]

$$C''_D(\omega_\nu) = \sum_{\mathbf{q}} |g_{\mathbf{q}}^e - g_{\mathbf{q}}^h|^2 \delta(\omega_\nu - \omega_{\mathbf{q}})$$

$$= 2\pi S_D \frac{\omega_\nu^4}{2\omega_c^3} \exp\left[-\omega_\nu/\omega_c\right] \tag{2}$$

where we use values for the Huang-Rhys factor $S_D = 0.05$ and cutoff frequency $\omega_c = 0.2$ THz. Note that the first line in Equation (2) is the general definition of the spectral density, and facilitates conversion between summation over wavevector $\mathbf{q}$ to an integral over continuous vibrational frequency ω_ν that accounts for any energy degeneracy in the case of multiple branches.

2.2. Impulsive Excitation

Dynamics of the above Hamiltonian in response to external driving are often obtained by perturbative solution of density matrix equations of motion,[36,37] but the expressions can be unwieldy for nonlinear responses while the dynamics of bath degrees of freedom are obscured. To obtain an exact solution for multidimensional spectroscopy of the spin-boson Hamiltonian described above, we apply a treatment by Vagov et al.[27] for impulsive excitation in terms of three generating functions:[38]

$$Y(\alpha_{\mathbf{q}}, \beta_{\mathbf{q}}, t) = \left\langle dc\, e^{\sum_{\mathbf{q}} \alpha_{\mathbf{q}} b_{\mathbf{q}}^\dagger} e^{\sum_{\mathbf{q}} \beta_{\mathbf{q}} b_{\mathbf{q}}} \right\rangle \tag{3}$$

$$C(\alpha_{\mathbf{q}}, \beta_{\mathbf{q}}, t) = \left\langle c^\dagger c\, e^{\sum_{\mathbf{q}} \alpha_{\mathbf{q}} b_{\mathbf{q}}^\dagger} e^{\sum_{\mathbf{q}} \beta_{\mathbf{q}} b_{\mathbf{q}}} \right\rangle \tag{4}$$

$$F(\alpha_{\mathbf{q}}, \beta_{\mathbf{q}}, t) = \left\langle e^{\sum_{\mathbf{q}} \alpha_{\mathbf{q}} b_{\mathbf{q}}^\dagger} e^{\sum_{\mathbf{q}} \beta_{\mathbf{q}} b_{\mathbf{q}}} \right\rangle \tag{5}$$

where $\alpha_{\mathbf{q}}$ and $\beta_{\mathbf{q}}$ are complex parameters introduced for deriving the equations of motion, and will be eliminated upon evaluating the spectroscopic observables. For this purpose, the first function Y returns the polarization:

$$P(t) = M^* Y(\alpha_{\mathbf{q}}, \beta_{\mathbf{q}}, t)\Big|_{\alpha_{\mathbf{q}} = \beta_{\mathbf{q}} = 0} \tag{6}$$

while the other two functions C and F return the electronic population and bath amplitude, respectively upon similar operations involving $\alpha_{\mathbf{q}}$ and $\beta_{\mathbf{q}}$.[27]

In the following, we begin by reiterating the solution for excitation by a single pulse derived in ref. [27]. By extending the two-pulse solutions presented in ref. [27] we then present the main result of this study, which is an expression for excitation by three pulses that describes multidimensional coherent spectroscopies. This expression will be demonstrated for two case studies, namely dynamics of polaron formation in electronic linewidths and coherent signatures of coupling to discrete bath modes.

3. Single-Pulse Excitation

We first consider the scenario of excitation by a single pulse of pulse area f_1 that arrives at $\tau = 0$ (see **Figure 1a**). For initial conditions of the system in its ground state and the bath at thermal equilibrium, the resultant polarization $P_1(\tau)$ was derived in ref. [27] as:

$$P_1(\tau) = \frac{i}{2} \sin(f_1) e^{-i\overline{\Omega}\tau} e^{i\mathbf{k}_1 \cdot \mathbf{r}} e^{-\gamma\tau}$$

$$\times \exp\left[\int \frac{C''(\omega_\nu)}{\omega_\nu^2} \left\{ (e^{-i\omega_\nu\tau} - 1) - N_\nu |(e^{-i\omega_\nu\tau} - 1)|^2 \right\} d\omega_\nu \right] \tag{7}$$

where $\overline{\Omega} = \Omega - \int \frac{C''(\omega_\nu)}{\omega_\nu^2} \omega_\nu d\omega_\nu$ incorporates the lattice reorganization energy, γ is a phenomenological homogeneous dephasing rate, $N_\nu = 1/(\exp[\hbar\omega_\nu/k_B\mathcal{T}] - 1)$ is the thermal distribution of the bath at a temperature $\mathcal{T}$, and the dipole moment M is set to unity for simplicity.

The Fourier transform of the temporal polarization $P_1(\omega_\tau)$ directly leads to a corresponding linear absorption spectrum:[24]

$$A(\omega_\tau) \propto -\mathrm{Re}\{iP_1(\omega_\tau)\} \tag{8}$$

simulated for three representative temperatures and plotted in the top panel of Figure 1b. The absorption spectrum exhibits a complex lineshape at the lowest temperature of 10 K that becomes gradually featureless up to 70 K. Besides the sharp zero-phonon line[39] (broadened by $\gamma = 0.1$ THz), the surrounding pedestal physically corresponds to inelastic scattering with low-frequency vibrations and is therefore a direct characterization of the spectral density.[40,41] In many realistic systems however, there is unavoidable disorder of the electronic resonance energy $\overline{\Omega}$ and the polarization must be convolved with the resonance energy distribution. Absorption spectra incorporating a Gaussian resonance energy distribution of width $\sigma = 30$ THz are plotted in the bottom panel of Figure 1b, whose intricate homogeneous
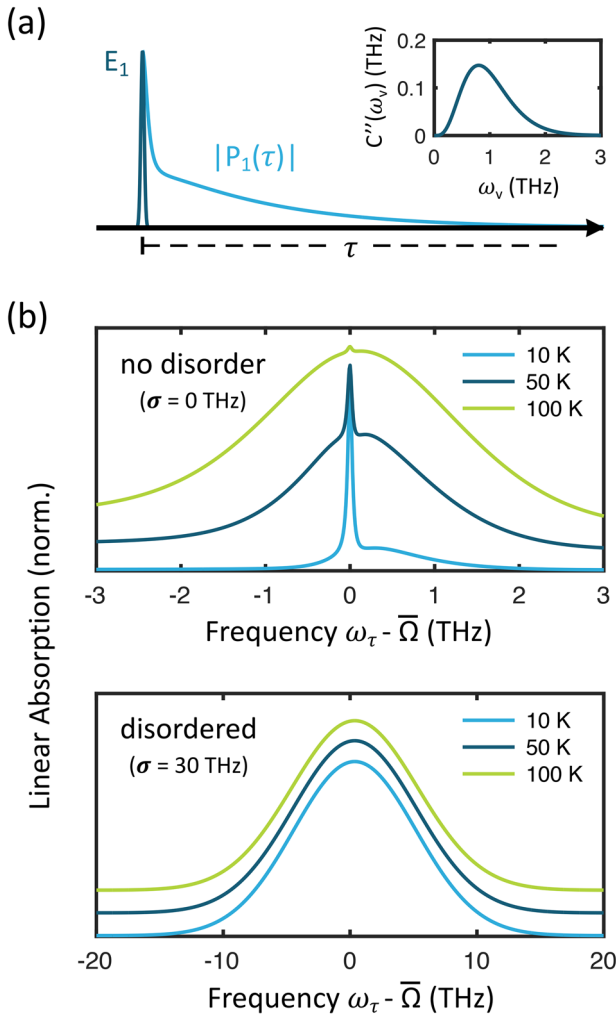
**ADVANCED
SCIENCE NEWS**

www.advancedsciencenews.com

**ADVANCED
QUANTUM
TECHNOLOGIES**

www.advquantumtech.com

Figure 1. a) Schematic of the single excitation pulse E_1, which impulsively excites a polarization $P_1(\tau)$, simulated for a temperature of 10 K and the parameters described in the text. b) Corresponding absorption spectra for three temperatures as indicated. Simulations are performed for both no disorder (top panel) and a Gaussian resonance energy distribution of width $\sigma = 30$ THz.

lineshapes have been completely obscured by the disorder.[42] Resolving these lineshapes in the presence of such electronic disorder is a primary motivation for applying multidimensional spectroscopy, which will be the focus of the remaining text.

4. Three-Pulse Excitation

We now consider the general scenario of excitation by three pulses $\{E_1, E_2, E_3\}$, with inter-pulse time delays $\{\tau, T\}$ and an emission time t (see **Figure 2a**). By sequential propagation of each generating function (described in the Supporting Information), one obtains numerous polarization terms that emit in unique phase-matched directions. Here, we focus on deriving an expression for the photon-echo signal most commonly measured in MDCS experiments (emitted with a wavevector $\mathbf{k}_{sig} = -\mathbf{k}_1 + \mathbf{k}_2 + \mathbf{k}_3$), and arrive at the main result of this study:

$$P_3^{echo}(\tau, T, t) = -\frac{i}{4} \sin(f_1) \sin(f_2) \sin(f_3) e^{i\overline{\Omega}(\tau - t)} e^{-i(\mathbf{k}_1 - \mathbf{k}_2 - \mathbf{k}_3)} e^{-\gamma(t+\tau)}$$

$$\times \exp\left[\int \frac{C''(\omega_\nu)}{\omega_\nu^2} \left\{ e^{-i\omega_\nu t} + e^{i\omega_\nu(T+\tau)} - e^{i\omega_\nu(\tau+T+t)} \right.\right.$$

$$+ e^{i\omega_\nu\tau} + e^{i\omega_\nu(T+t)} - e^{i\omega_\nu T} - 2 - N_\nu |e^{-i\omega_\nu(\tau+T)}$$

$$\left.\left. - e^{-i\omega_\nu(\tau+T+t)} + e^{-i\omega_\nu\tau} - 1|^2 \right\} d\omega_\nu \right] \qquad (9)$$

which is immediately seen to be more compact than the usual perturbative expression.[36,37,43] We point out two additional advantages of this expression. First, that this expression simplifies interpretation by separating the zero-temperature dynamics of the coupled system and bath (first bracketed term) from the stimulated dynamics induced by thermal occupation of the bath (second bracketed term). Second, that corresponding dynamics of the electronic and vibrational populations can be directly obtained from the generating functions C and F.[27] In addition to this rephasing term of the nonlinear polarization, a corresponding non-rephasing polarization (emitted with a wavevector $\mathbf{k}_{sig} = \mathbf{k}_1 - \mathbf{k}_2 + \mathbf{k}_3$) is often desired as well, for example to generate absorptive 2-D spectra.[24] This non-rephasing polarization may be found in an analogous fashion, and is presented in the Supporting Information. We perform demonstrative simulations of Equation (9) in the following.

As shown in Figure 2a, the polarization $|P_3^{echo}(\tau, T, t)|$ exhibits a characteristic revival at $t = \tau$ due to 'rephasing' of the disordered Bloch vectors,[20] whose width is the inverse of the disorder linewidth σ. By integrating Equation (9) along the emission time t, one can describe integrated photon-echo experiments as shown in Figure 2b (simulated for the same Debye spectral density and disorder linewidth σ as above). As observed in experiments, such as on quantum dots,[44,45] quantum wells,[46] and 2-D van der Waals materials,[47] the dephasing along τ exhibits both slow and fast decay components, corresponding to dephasing of the zero-phonon line and from bath-induced scattering, respectively. With increasing temperature the fast decay component dominates, corresponding to the growth of the pedestal in Figure 1b.

The simulations in Figure 2b demonstrate how integrated photon-echo spectroscopy is able to resolve homogeneous dephasing dynamics in the presence of disorder. However, this technique suffers from two primary limitations. First, with the goal of characterizing the spectral density in mind, subtle differences in the bath-induced fast decay component are difficult to interpret in the time-domain. Second, the dephasing dynamics probed by integrated techniques necessarily measure an ensemble-averaged quantity, which can obscure important variations across the disordered ensemble. Both of these limitations may be circumvented by spectrally-resolving the nonlinear absorption and emission processes, as well as their correlations, a primary capability of MDCS.

To correlate absorption and emission by MDCS, one measures the polarization P_3^{echo} along two time delays $\{\tau, t\}$ and simultaneous Fourier transform along both time axes returns a 2-D spectrum. 2-D spectra simulated via Equation (9) are shown in Figure 2c, in which the vertical 'absorption' and horizontal 'emission' frequency axes correspond to the Fourier conjugate axes of τ

**ADVANCED
SCIENCE NEWS**

www.advancedsciencenews.com

**ADVANCED
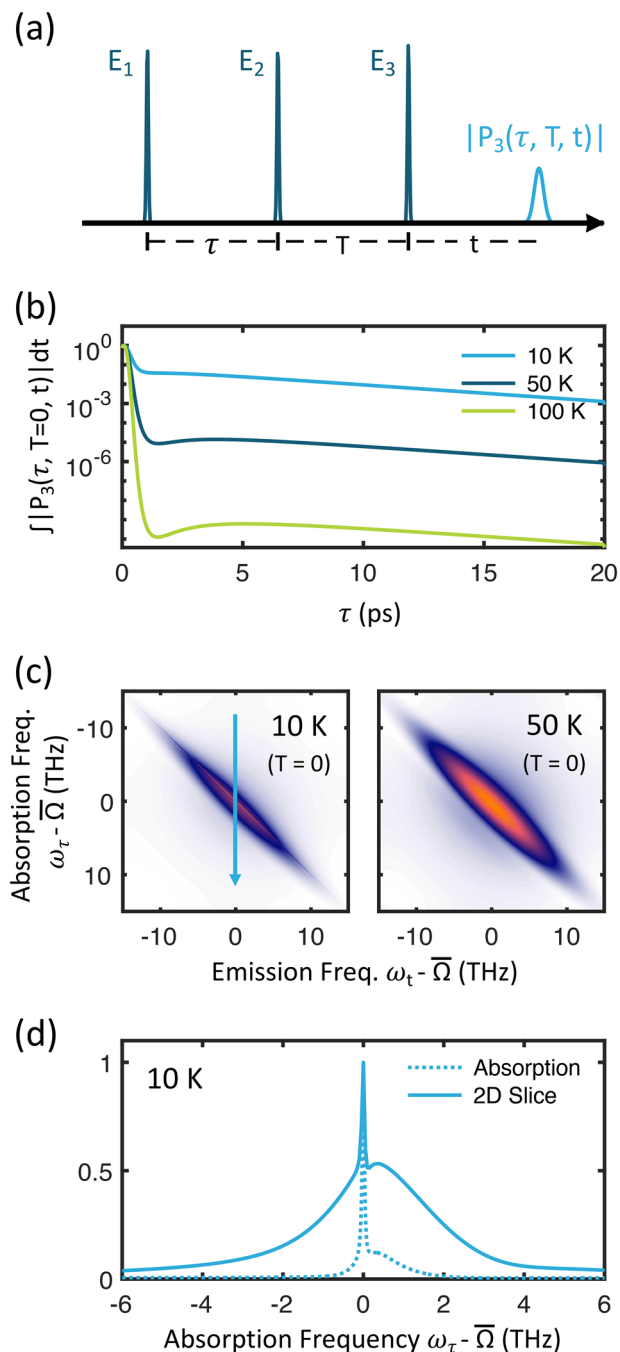QUANTUM
TECHNOLOGIES**

www.advquantumtech.com

Figure 2. a) Schematic of the three excitation pulses $\{E_1, E_2, E_3\}$ which impulsively excite a polarization $P_3(\tau, T, t)$. b, c) Simulations of (b) integrated photon-echo and (c) MDCS performed for a disorder linewidth of $\sigma = 30$ THz and $T = 0$. d) Comparison at 10 K of an absorption spectrum (no disorder) to the 2-D spectrum slice taken along the blue arrow in (c). A nonlinear enhancement of the pedestal, arising from system-bath coupling, is observed in the nonlinear 2-D spectrum.

and t, respectively. The utility of such a 2-D spectrum comes from the fact that the disorder lineshape and the homogeneous spectral lineshape are projected into orthogonal directions,[48] in principle permitting a measurement of the spectral density across the resonance frequency distribution.[49]

To illustrate this idea, we take a vertical slice of the spectrum at 10 K to obtain a pseudo-absorption spectrum, and plot this in Figure 2d with the linear absorption spectrum in Figure 1b (with no disorder) for comparison. Besides a clear correspondence between the two lineshapes, the pedestal feature is notably more prominent in the slice, which reflects a nonlinear enhancement of system-bath coupling signatures in 2-D spectra. Indeed, MDCS was recently applied to colloidal CdSe quantum dots at cryogenic temperatures for this purpose,[41] demonstrating the technique as a direct, sensitive probe of the spectral density of system-bath coupling.

5. Two Case Studies

We now demonstrate the utility of Equation (9) by reproducing observables in two exemplary experiments, namely in studying polaron formation through 2-D lineshape analysis, and resolving coherent phonon dynamics using MDCS. Both of these case studies are performed on excitons in a host crystal lattice, but have direct analogues to any generic open quantum system characterized by a spectral density with a low-frequency continuum and discrete high-frequency mode, respectively.

5.1. Polaron Formation Dynamics

The concept of a non-equilibrium bath amplitude following excitation of a system is ubiquitous. In molecular systems this is clearly represented in a displaced oscillator model,[33] in which transition to an excited state potential changes the bath energy minimum. In condensed systems (with a lattice) a continuum of bath modes of varying momenta are simultaneously displaced, resulting in a standing wave surrounding the excitation. The resulting quasiparticle incorporating a lattice potential well is known as a polaron,[50] a concept, which has proved central to understanding a wide swath of functional materials.[51]

In a recent study by Seiler et al.,[52] MDCS was applied to CsPbI$_3$ nanocrystals toward resolving polaron formation dynamics. Although the experiment was performed at room temperature, where exciton lineshapes are relatively featureless with the linewidth being its sole characteristic, polaron formation may be inferred by tracking the linewidth as a function of intermediate time-delay T. With increasing T, absorption and emission frequencies become increasingly uncorrelated due to lattice relaxation, resulting in an effective broadening of the exciton lineshape.[53]

In **Figure 3a**, we plot a 2-D spectrum at room temperature and extract the resonance linewidth from vertical slices taken along the blue arrow indicated (while sufficient for characterizing polaron formation, we note that quantifying homogeneous linewidths requires extraction of the anti-diagonal linewidth[48]). The linewidth is observed to vary as a function of T, which is quantified in Figure 3b with the full-width at half max as a function of T. The linewidth increases rapidly in the first 400 fs, very similar to the behavior attributed to polaron formation observed in ref. [52], and then stabilizes after a picosecond. We note that at low temperatures, polaron formation additionally manifests in evolution of the pedestal feature around the zero-phonon line, becoming more symmetric as vibrational absorption and emission processes equilibrate in the excited state potential.[54,55]
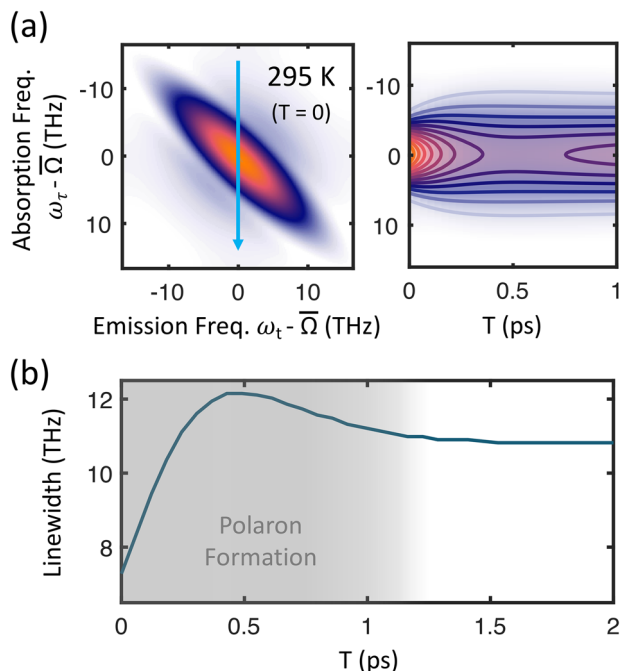
**ADVANCED
SCIENCE NEWS**

www.advancedsciencenews.com

**ADVANCED
QUANTUM
TECHNOLOGIES**

www.advquantumtech.com

Figure 3. a) Simulated 2-D spectrum at room temperature and $T = 0$. Blue arrow indicates position of slices shown in the right panel as a function of intermediate delay T. b) Full-width at half max extracted from slices in (a), which changes rapidly in the first picosecond, indicating polaron formation.

5.2. Coherent Phonon Dynamics

Up to this point, we have considered only a Debye contribution to the spectral density that results in overdamped, incoherent dynamics. However, discrete molecular or lattice vibrations may also be incorporated into the spectral density, for example through a Lorentzian contribution of the form:[36,37]:

$$C_L''(\omega_\nu) = \frac{2^{3/2} S_L \omega_L^3 \gamma_L \omega_\nu}{(\omega_\nu^2 - \omega_L^2)^2 + 2\gamma_L^2 \omega_\nu^2} \tag{10}$$

where, we use the values for the Huang-Rhys factor $S_L = 0.05$, the mode frequency $\omega_L = 6$ THz, and a damping rate $\gamma_L = 0.75$ THz. These values are chosen to mimic exciton coupling to the longitudinal-optical (LO) phonon in CdSe, a simple model system that has been extensively studied.[56]

Exciton coupling to LO phonons in CdSe quantum dots was studied by us[57] and others[58–61] using MDCS, in which LO phonons manifested as clear sidebands adjacent to the exciton peak in the 2-D spectra. A nonlinear analogue to phonon replicas[56,62] in linear absorption or luminescence spectra, these sidebands additional exhibit coherent dynamics that provide direct insight into the microscopic parameters of exciton-phonon coupling.

In **Figure 4a**, we present 2-D spectra simulated at 10 K which incorporate both the Debye contribution to the spectral density in Equation (2) as well as the Lorentzian contribution in Equation (10). In agreement with experiment, two sidebands are observed above and below the primary exciton peak whose ratio
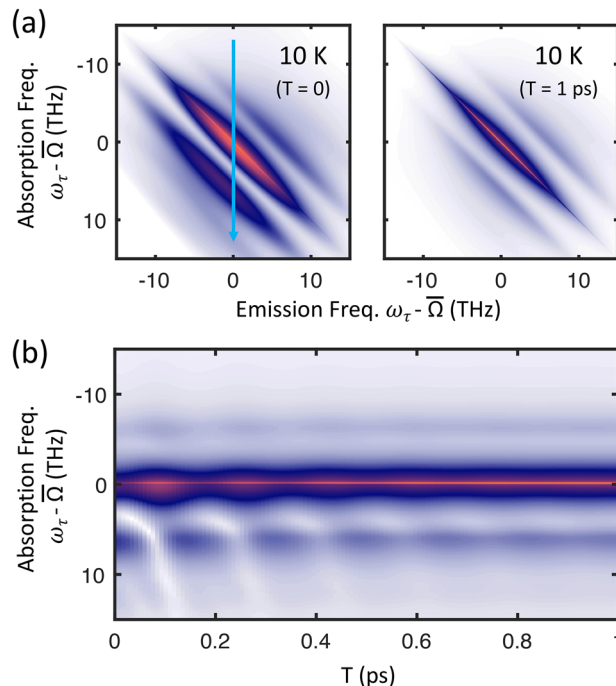

Figure 4. a) 2-D spectra simulated for a spectral density incorporating a discrete phonon mode. The blue arrow indicates the location of the slices plotted in (b). b) Dependence of the vertical slice indicated in (a) as a function of intermediate delay T. Strong coherent oscillations of the lower sideband are observed with minimal modulation of the upper sideband.

depends on the intermediate delay T. To examine the dynamics more closely, slices are taken along the blue arrow in (a) as a function of T and plotted in Figure 4b. Indeed, strong coherent oscillations are observed of the lower sideband in strong agreement with experiment. The difference in coherent dynamics between the upper and lower sidebands can be intuitively understood by associating the upper sideband to initial absorption into a stationary vibrational ground state and the lower sideband to initial absorption into a vibrational excited state that launches subsequent coherent dynamics.

We emphasize again that the above simulations and referenced experiments are all performed in the presence of a large distribution of resonance energies, underscoring the powerful ability of MDCS to extract information about the spectral density even in the presence of dominant disorder broadening.

6. Conclusion

In summary, we have presented an exact and compact expression for multi-dimensional spectroscopy of a spin-boson Hamiltonian. The expression was derived from a generating function approach by Vagov et al.,[27] originally developed for linear and integrated two-pulse four-wave mixing experiments. We have demonstrated its validity in two case studies from literature that study continuum low-frequency and discrete high-frequency components of the spectral density, respectively. These are a study of polaron formation dynamics through an ultrafast increase in transition linewidth,[52] and a study of coherent exciton-phonon coupling dynamics[57–61] by MDCS.

**ADVANCED
SCIENCE NEWS**

www.advancedsciencenews.com

**ADVANCED
QUANTUM
TECHNOLOGIES**

www.advquantumtech.com

The expression derived here successfully reproduces both experimental observables.

There are of course many systems that require a more sophisticated approach to model, for example those with multiple participating quantum states,[63–66] higher-order system-bath couplings,[67] or a bath with strong anharmonicities.[68] Excitation schemes that use pulses that break the impulsive approximation also will require numerical approaches. Nevertheless, the expression presented here is expected to apply to a broad range of systems, and greatly simplify simulating MDCS of open quantum systems.

Supporting Information

Acknowledgements

Conflict of Interest

The authors declare no conflict of interest.

Data Availability Statement

Data sharing is not applicable to this article as no new data were created or analyzed in this study.

Keywords

[1] *The Theory of Open Quantum Systems*, (Eds: H.-P. Breuer, F. Petruccione), Oxford University Press, Oxford, **2007**.

[2] *Quantum Noise: A Handbook of Markovian and Non-Markovian Quantum Stochastic Methods with Applications to Quantum Optics*, (Eds.: C. Gardiner, P. Zoller), Springer Berlin, Berlin, **2004**.

[3] *Quantum Effects in Biology*, (Eds.: M. Mohseni, Y. Omar, G. S. Engel, M. B. Plenio), Cambridge University Press, Cambridge, **2014**.

[4] I. Rotter, J. P. Bird, *Rep. Prog. Phys.* **2015**, *78*, 114001.

[5] T. Mori, *Annu. Rev. Condens. Matter Phys.* **2023**, *14*, 35.

[6] D. M. Reich, N. Katz, C. P. Koch, *Sci. Rep.* **2015**, *5*, 12430.

[7] Z.-X. Man, Y.-J. Xia, R. Lo Franco, *Phys. Rev. A* **2015**, *92*, 012315.

[8] M. Miller, K.-D. Wu, M. Scalici, J. Kołodyński, G.-Y. Xiang, C.-F. Li, G.-C. Guo, A. Streltsov, *New J. Phys.* **2022**, *24*, 053022.

[9] *Optical Properties of Solids*, (Ed.: M. Fox), Oxford University Press, Oxford, **2010**.

[10] J. Fidy, M. Laberge, A. D. Kaposi, J. M. Vanderkooi, *Biochim. biophys. acta, Prot. struct. mol. enzymol.* **1998**, *1386*, 331.

[11] M. Wendling, T. Pullerits, M. A. Przyjalgowski, S. I. E. Vulto, T. J. Aartsma, R. van Grondelle, H. van Amerongen, *J. Phys. Chem. B* **2000**, *104*, 5825.

[12] S. T. Cundiff, *Opt. Express* **2008**, *16*, 4639.

[13] *Persistent Spectral Hole-Burning: Science and Applications*, (Ed.: W. E. Moerner), Springer Berlin, Berlin, **1988**.

[14] V. O. Lorenz, S. T. Cundiff, *Phys. Rev. Lett.* **2005**, *95*, 163601.

[15] G. Hétet, M. Hosseini, B. M. Sparkes, D. Oblak, P. K. Lam, B. C. Buchler, *Opt. Lett.* **2008**, *33*, 2323.

[16] M. Cho, N. F. Scherer, G. R. Fleming, S. Mukamel, *J. Chem. Phys.* **1992**, *96*, 5618.

[17] T. Jakubczyk, V. Delmonte, M. Koperski, K. Nogajewski, C. Faugeras, W. Langbein, M. Potemski, J. Kasprzak, *Nano Lett.* **2016**, *16*, 5333.

[18] A. Liu, S. T. Cundiff, D. B. Almeida, R. Ulbricht, *Mater. Quantum Technol.* **2021**, *1*, 025002.

[19] S. T. Cundiff, S. Mukamel, *Phys. Today* **2013**, *66*, 44.

[20] H. Li, B. Lomsadze, G. Moody, C. Smallwood, S. Cundiff, *Optical Multidimensional Coherent Spectroscopy*, Oxford University Press, Oxford, **2023**.

[21] A. Liu, D. B. Almeida, L. A. Padilha, S. T. Cundiff, *J. Phys. Mater.* **2022**, *5*, 021002.

[22] S. Mukamel, *Principles of Nonlinear Optical Spectroscopy*, Oxford University Press, Oxford, **1999**.

[23] M. Cho, *Two-Dimensional Optical Spectroscopy*, CRC Press, Boca Raton, **2009**.

[24] P. Hamm, M. Zanni, *Concepts and Methods of 2D Infrared Spectroscopy*, Cambridge University Press, Cambridge, **2012**.

[25] Y. Tanimura, K. Okumura, *J. Chem. Phys.* **1997**, *106*, 2078.

[26] Z. Zhang, K. L. Wells, M. T. Seidel, H.-S. Tan, *J. Phys. Chem. B* **2013**, *117*, 15369.

[27] A. Vagov, V. M. Axt, T. Kuhn, *Phys. Rev. B* **2002**, *66*, 165312.

[28] A. J. Leggett, S. Chakravarty, A. T. Dorsey, M. P. A. Fisher, A. Garg, W. Zwerger, *Rev. Mod. Phys.* **1987**, *59*, 1.

[29] T. Calarco, A. Datta, P. Fedichev, E. Pazy, P. Zoller, *Phys. Rev. A* **2003**, *68*, 012310.

[30] M. Schlosshauer, *Decoherence: and the Quantum-To-Classical Transition*, Springer Berlin, Heidelberg, **2007**.

[31] A. Chenu, S.-Y. Shiau, M. Combescot, *Phys. Rev. B* **2019**, *99*, 014302.

[32] G. R. Fleming, M. Cho, *Annu. Rev. Phys. Chem.* **1996**, *47*, 109.

[33] A. Nitzan, *Chemical Dynamics in Condensed Phases: Relaxation, Transfer, and Reactions in Condensed Molecular Systems*, Oxford University Press, Oxford, **2006**.

[34] H. Wang, X. Song, D. Chandler, W. H. Miller, *J. Chem. Phys.* **1999**, *110*, 4828.

[35] P. Kjellberg, B. Brüggemann, T. Pullerits, *Phys. Rev. B* **2006**, *74*, 024303.

[36] J. Seibt, T. Hansen, T. Pullerits, *J. Phys. Chem. B* **2013**, *117*, 11124.

[37] V. Butkus, L. Valkunas, D. Abramavicius, *J. Chem. Phys.* **2012**, *137*, 044513.

[38] V. M. Axt, S. Mukamel, *Rev. Mod. Phys.* **1998**, *70*, 145.

[39] D. Hsu, J. L. Skinner, *J. Chem. Phys.* **1984**, *81*, 1604.

[40] B. Krummheuer, V. M. Axt, T. Kuhn, *Phys. Rev. B* **2002**, *65*, 195313.

[41] A. Liu, D. B. Almeida, W.-K. Bae, L. A. Padilha, S. T. Cundiff, *J. Phys. Chem. Lett.* **2019**, *10*, 6144.

[42] A. Liu, L. G. Bonato, F. Sessa, D. B. Almeida, E. Isele, G. Nagamine, L. F. Zagonel, A. F. Nogueira, L. A. Padilha, S. T. Cundiff, *J. Chem. Phys.* **2019**, *151*, 191103.

[43] J. Seibt, T. Pullerits, *J. Phys. Chem. C* **2013**, *117*, 18728.

[44] F. Masia, N. Accanto, W. Langbein, P. Borri, *Phys. Rev. Lett.* **2012**, *108*, 087401.

**ADVANCED
SCIENCE NEWS**

www.advancedsciencenews.com

**ADVANCED
QUANTUM
TECHNOLOGIES**

www.advquantumtech.com

[45] M. A. Becker, L. Scarpelli, G. Nedelcu, G. Rainò, F. Masia, P. Borri, T. Stöferle, M. V. Kovalenko, W. Langbein, R. F. Mahrt, *Nano Lett.* **2018**, *18*, 7546.

[46] L. Langer, S. V. Poltavtsev, I. A. Yugova, M. Salewski, D. R. Yakovlev, G. Karczewski, T. Wojtowicz, I. A. Akimov, M. Bayer, *Nat. Photonics* **2014**, *8*, 851.

[47] P. Dey, J. Paul, Z. Wang, C. E. Stevens, C. Liu, A. H. Romero, J. Shan, D. J. Hilton, D. Karaiskaj, *Phys. Rev. Lett.* **2016**, *116*, 127402.

[48] M. E. Siemens, G. Moody, H. Li, A. D. Bristow, S. T. Cundiff, *Opt. Express* **2010**, *18*, 17699.

[49] A. Liu, G. Nagamine, L. G. Bonato, D. B. Almeida, L. F. Zagonel, A. F. Nogueira, L. A. Padilha, S. T. Cundiff, *ACS Nano* **2021**, *15*, 6499.

[50] D. Emin, *Polarons*, Cambridge University Press, Cambridge, **2013**.

[51] C. Franchini, M. Reticcioli, M. Setvin, U. Diebold, *Nat. Rev. Mater.* **2021**, *6*, 560.

[52] H. Seiler, S. Palato, C. Sonnichsen, H. Baker, E. Socie, D. P. Strandell, P. Kambhampati, *Nat. Commun.* **2019**, *10*, 4962.

[53] R. Singh, G. Moody, M. E. Siemens, H. Li, S. T. Cundiff, *J. Opt. Soc. Am. B* **2016**, *33*, C137.

[54] A. Krügel, A. Vagov, V. M. Axt, T. Kuhn, *Phys. Rev. B* **2007**, *76*, 195302.

[55] D. Wigger, V. Karakhanyan, C. Schneider, M. Kamp, S. Höfling, P. Machnikowski, T. Kuhn, J. Kasprzak, *Opt. Lett.* **2020**, *45*, 919.

[56] A. M. Kelley, *J. Chem. Phys.* **2019**, *151*, 140901.

[57] A. Liu, D. B. Almeida, W. K. Bae, L. A. Padilha, S. T. Cundiff, *Phys. Rev. Lett.* **2019**, *123*, 057403.

[58] J. R. Caram, H. Zheng, P. D. Dahlberg, B. S. Rolczynski, G. B. Griffin, A. F. Fidler, D. S. Dolzhnikov, D. V. Talapin, G. S. Engel, *J. Phys. Chem. Lett.* **2014**, *5*, 196.

[59] R. Wang, X.-y. Huang, C.-f. Zhang, X.-y. Wang, M. Xiao, *Chin. J. Chem. Phys.* **2017**, *30*, 637.

[60] T. A. Gellen, J. Lem, D. B. Turner, *Nano Lett.* **2017**, *17*, 2809.

[61] Z. Wang, A. Hedse, E. Amarotti, N. Lenngren, K. Žídek, K. Zheng, D. Zigmantas, T. Pullerits, *J. Chem. Phys.* **2022**, *157*, 014201.

[62] A. Liu, D. B. Almeida, S. T. Cundiff, L. A. Padilha, *Electron. Struct.* **2023**, *5*, 033001.

[63] D. B. Turner, K. A. Nelson, *Nature* **2010**, *466*, 1089.

[64] A. Liu, D. B. Almeida, L. G. Bonato, G. Nagamine, L. F. Zagonel, A. F. Nogueira, L. A. Padilha, S. T. Cundiff, *Sci. Adv.* **2021**, *7*, eabb3594.

[65] A. Liu, *Nanomaterials* **2022**, *12*, 5.

[66] J. Lüttig, S. Mueller, P. Malý, J. J. Krich, T. Brixner, *J. Phys. Chem. Lett.* **2023**, *14*, 7556.

[67] R. F. Loring, *Annu. Rev. Phys. Chem.* **2022**, *73*, 273.

[68] K. Okumura, Y. Tanimura, *J. Chem. Phys.* **1996**, *105*, 7294.